The Plant Cell, Vol. 26: 3680–3692, September 2014, www.plantcell.org © 2014 American Society of Plant Biologists. All rights reserved.

Arabidopsis thaliana RNase H2 Deficiency Counteracts the Needs for the WEE1 Checkpoint Kinase but Triggers Genome Instability[C][W]

Pooneh Kalhorzadeh,[a,b] Zhubing Hu,[a,b] Toon Cools,[a,b] Simon Amiard,[c] Eva-Maria Willing,[d] Nancy De Winne,[a,b] Kris Gevaert,[e,f] Geert De Jaeger,[a,b] Korbinian Schneeberger,[d] Charles I. White,[c] and Lieven De Veylder[a,b,1]

[a] Department of Plant Systems Biology, Flanders Institute for Biotechnology (VIB), B-9052 Ghent, Belgium
[b] Department of Plant Biotechnology and Bioinformatics, Ghent University, B-9052 Ghent, Belgium
[c] Génétique, Reproduction et Développement, Centre National de la Recherche Scientifique, Unité Mixte de Recherche 6293-Clermont Université-Institut National de la Santé et de la Recherche Médicale U1103, F-63177 Aubière, France
[d] Department for Plant Developmental Biology, Max Planck Institute for Plant Breeding Research, 50829 Cologne, Germany
[e] Department of Medical Protein Research, Flanders Institute for Biotechnology (VIB), B-9000 Ghent, Belgium
[f] Department of Biochemistry, Ghent University, B-9000 Ghent, Belgium

The WEE1 kinase is an essential cell cycle checkpoint regulator in *Arabidopsis thaliana* plants experiencing replication defects. Whereas under non-stress conditions *WEE1*-deficient plants develop normally, they fail to adapt to replication inhibitory conditions, resulting in the accumulation of DNA damage and loss of cell division competence. We identified mutant alleles of the genes encoding subunits of the ribonuclease H2 (RNase H2) complex, known for its role in removing ribonucleotides from DNA-RNA duplexes, as suppressor mutants of *WEE1* knockout plants. RNase H2 deficiency triggered an increase in homologous recombination (HR), correlated with the accumulation of γ-H2AX foci. However, as HR negatively impacts the growth of *WEE1*-deficient plants under replication stress, it cannot account for the rescue of the replication defects of the *WEE1* knockout plants. Rather, the observed increase in ribonucleotide incorporation in DNA indicates that the substitution of deoxynucleotide with ribonucleotide abolishes the need for WEE1 under replication stress. Strikingly, increased ribonucleotide incorporation in DNA correlated with the occurrence of small base pair deletions, identifying the RNase H2 complex as an important suppressor of genome instability.

INTRODUCTION

Faithful duplication of the genome is important for error-free transmission of the genetic information from one generation to the next. Because during growth and development the DNA is prone to damage induced by environmental stress and endogenous factors, DNA synthesis is accompanied by several quality checks, called checkpoints, which arrest the cell cycle for DNA repair upon damage. Similar to other organisms, in plants, two central players of this DNA damage response are the Ataxia Telangiectasia Mutated (ATM) and ATM- and RAD3-related (ATR) protein kinases. In general, ATR is triggered by stalled replication forks and single-stranded DNA (ssDNA), whereas ATM is activated by double-strand breaks (DSBs) (Garcia et al., 2003; Culligan et al., 2004, 2006; Ricaud et al., 2007; Ciccia and Elledge, 2010). In animals, DNA stress checkpoint activation by ATM and ATR triggers eventually a transient or permanent cell cycle arrest through the phosphorylation of a number of downstream proteins, including the CDC25 phosphatase and WEE1 kinase, which operate as the on and off switches of cyclin-dependent kinase (CDK) activity (Harper and Elledge, 2007).

Plants lack an orthologous *CDC25* gene (Boudolf et al., 2006) but possess a homolog of the WEE1 protein kinase (Sun et al., 1999; Sorrell et al., 2002; Gonzalez et al., 2004). *Arabidopsis thaliana WEE1* transcript levels are strongly induced upon treatment with replication-inhibitory drugs in an ATR-dependent manner. Moreover, whereas *WEE1* knockout (*WEE1*^{KO}) mutants show a wild-type phenotype under normal growth conditions, they are hypersensitive to drugs inducing replication stress (De Schutter et al., 2007). Molecular analysis revealed that absence of WEE1 results in altered S-phase kinetics, suggesting a role in the adaptation of the DNA replication rate in response to replication defects. The inability to do so eventually triggers premature differentiation and a cell death phenotype within the root meristem (Cools et al., 2011).

Replication stress can be triggered by the application of hydroxyurea (HU), inhibiting the activity of the ribonucleotide reductase (RNR) enzyme that is responsible for the reduction of ribonucleotides (rNTPs) to deoxyribonucleotides (dNTPs) and consequently limiting dNTP availability for DNA polymerases. These polymerases have evolved mechanisms to efficiently recognize and incorporate dNTPs, but not rNTPs, into the genome. This is achieved through sugar-type discrimination, as dNTPs possess deoxyribose, whereas ribose is the sugar

[1] Address correspondence to lieven.deveylder@psb.vib-ugent.be.
The author responsible for distribution of materials integral to the findings presented in this article in accordance with the policy described in the Instructions for Authors (www.plantcell.org) is: Lieven De Veylder (lieven.deveylder@psb.vib-ugent.be).
[C] Some figures in this article are displayed in color online but in black and white in the print edition.
[W] Online version contains Web-only data.
www.plantcell.org/cgi/doi/10.1105/tpc.114.128108

backbone of rNTPs (Brown and Suo, 2011). However, because rNTP levels are 10- to 2000-fold higher than dNTP levels (Ferraro et al., 2010; Nick McElhinny et al., 2010b), DNA polymerases may misincorporate rNTPs into genomic DNA every 10,000th to 100,000th nucleotide, making ribonucleoside monophosphate (rNMP) the most prevalent aberrant nucleotide occurring in DNA (Nick McElhinny et al., 2010a, 2010b; Reijns et al., 2012; Clausen et al., 2013). Ribonucleotides have a reactive 2'OH on the sugar part and this makes them more sensitive to strand cleavage, resulting in genome instability (Nick McElhinny et al., 2010a). Therefore, organisms evolved a repair pathway, called ribonucleotide excision repair, which is initiated by ribonucleases H (RNase H) that specifically catalyzes the cleavage of RNA in DNA-RNA duplexes (Stein and Hausen, 1969). There are two main types of RNase H. Type 1 RNase H (RNase H1) needs at least four sequential rNMPs for recognition and cleavage to occur, while type 2 (RNase H2) is able to cut even single rNMPs and is the only enzyme known to hydrolyze ribonucleotides misincorporated during genomic replication (Cerritelli and Crouch, 2009; Bubeck et al., 2011). When a single rNTP is incorporated in DNA, RNase H2 incises the DNA 5′ of the ribonucleotide, which produces DNA containing 3′ hydroxyl and 5′ phospho-ribonucleotide ends. Upon DNA replication by the POL δ and/or POL ε polymerases, the ribonucleotide is displaced and the resulting flap is excised by the FEN1 and/or EXO1 exonucleases, followed by ligation of the nick through the LIG1 ligase (Rydberg and Game, 2002; Sparks et al., 2012; Williams et al., 2012).

Here, we report that a mutation within the catalytic subunit of the RNase H2 complex was found to partially overcome the replication phenotype of *WEE1*^{KO} plants. Similarly, the mutation of the regulatory subunits of the RNase H2 complex rescued *WEE1*-deficient plants under replication stress. Rather than the observed increase in homologous recombination, the ability to overcome replication stress was found to correlate with an increased incorporation of rNMPs in DNA. This substitution of dNTPs with rNTPs restored replication kinetics of the *WEE1*^{KO} plants but resulted in replication errors, highlighting the need for RNase H2 activity to maintain genome stability.

RESULTS

A Mutation in the *RNase H2 Subunit A* Gene Rescues HU Hypersensitivity of *WEE1*^{KO} Plants

WEE1^{KO} seedlings (*wee1-1*) show a strong inhibition of root growth when grown on HU-containing medium (Figures 1A to 1C). To identify complementing mutations, an ethyl methanesulfonate-mutagenized *wee1-1* seed stock was screened in the M2 generation for restored root growth in the presence of 0.75 mM HU. Among the identified mutants, the *triffid1-1* (*trd1-1*) *wee1-1* mutant resulted in a partial recovery of root growth (Figures 1A to 1C) and an almost complete inhibition of the cell death phenotype (Figures 1D and 1E), as observed by the decrease in number of fluorescent cells upon treatment with propidium iodide, a fluorescent dye that outlines the walls of living cells but also penetrates through the plasma membrane of dead cells. The root meristem size of the different genotypes was measured by counting the meristematic cortex cells, which showed that under control growth conditions, there was no statistically significant difference between the wild-type (Columbia-0 [Col-0]) and the *wee1-1* and *wee1-1 trd1-1* mutant plants (Figures 1D and 1F). In the presence of HU, the number of dividing cortex cells was clearly reduced in *wee1-1* plants compared with wild-type seedlings (Figures 1E and 1F), whereas the meristem size of *wee1-1 trd1-1* mutants did differ significantly from that of wild-type plants.

Through next-generation sequencing-based gene mapping, the underlying mutation in the *trd1-1* mutant was pinpointed to a base pair change at codon position 584 of the *At2g25100* gene, resulting in a glycine (GGA) to glutamic acid (GAA) substitution (Figure 2A). This base pair change was confirmed by direct sequencing of the original mutant. The *At2g25100* gene is annotated as the catalytic subunit A of the RNase H2 protein complex. The amino acid change is located in a conserved domain (Figure 2B), directly next to a tyrosine finger that is pivotal for substrate binding (Rychlik et al., 2010), indicating that the mutant allele most probably encodes a nonfunctional protein. To confirm this hypothesis, we analyzed an available putative knockout line (GABI-139H04, nominated hereafter *trd1-2*) harboring a T-DNA insertion in intron 3 (Figure 2A). The *trd1-2* mutation was crossed in *wee1-1* plants and tested for HU hypersensitivity. Root growth analysis showed that the *trd1-2* mutation partially rescued the HU hypersensitivity of *WEE1*^{KO} mutants (Figures 1A to 1C). Similarly, the root cell death phenotype was suppressed in the double mutant, confirming that it is a lack of RNase H2 subunit A activity that rescues the replication defect of the WEE1 checkpoint mutant.

The Plant RNase H2 Complex Holds Three Subunits

TRD1-interacting proteins were screened for by tandem affinity purification (TAP) using cell cultures (Supplemental Data Set 1). Under control conditions the RNase H2 subunit A pulled down proteins homologous to the regulatory B and C subunits of the RNase H2 complex from other species (Figures 3A; Supplemental Data Set 2), revealing that the *Arabidopsis* RNase H2 complex comprises three subunits. The interaction between the three RNase H2 subunits was confirmed by reverse TAP experiments using the subunit B or subunit C as bait. Intriguingly, when performing TAP in the presence of HU, the thymidine kinase and the large subunit of ribonucleotide reductase 1 also were isolated (Figure 3B; Supplemental Data Set 2). Through yeast two-hybrid interaction assays, a direct connection could be detected only between the RNase H2 B and C subunits (Figure 3C), suggesting that most interactions between the different subunits occur through cooperative binding.

To check whether plants deficient in RNase H2 subunit B and C could revert the *wee1-1* mutant phenotype, T-DNA insertion lines of both genes were identified. Similar to the *trd1* mutants, absence of the RNase H2 subunit B or C rescued the HU hypersensitivity of the *WEE1*^{KO} line (Supplemental Figure 1).

RNase H2 Subunit A Mutants Display Constitutive High Recombination Rates

To better understand how the lack of RNase H2 activity overcomes the replication defects of *WEE1*^{KO} plants, an RNA sequencing experiment was conducted, comparing the transcriptome of

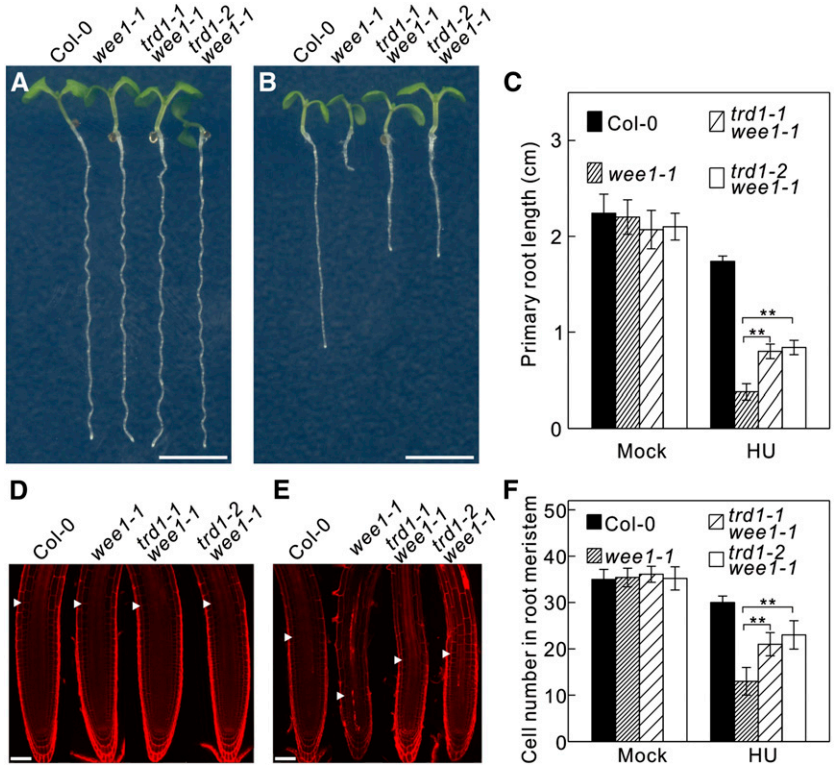

Figure 1. A Mutation in the Catalytic Subunit of the RNase H2 Complex Partially Rescues HU Hypersensitivity of *WEE1*^{KO} Plants.

(A) and **(B)** Root growth of 7-d-old wild-type (Col-0) and *wee1-1*, *trd1-1 wee1-1*, and *trd1-2 wee1-1* mutant plants grown on control medium **(A)** or medium supplemented with 0.75 mM HU **(B)**. Bar = 0.5 cm.

(C) Quantification of the root length of plants shown in **(A)** and **(B)**. Data represent mean ± SD ($n > 10$, **P value < 0.01, two-sided Student's *t* test).

(D) and **(E)** Representative confocal microscopy images of plants shown in **(A)** and **(B)** stained with propidium iodide. Arrowheads indicate the meristem size based on the cortical cell length. Bar = 50 μm.

(F) Number of meristematic cortex cells. Data represent mean ± SD ($n > 10$, **P value < 0.01, two-sided Student's *t* test).

[See online article for color version of this figure.]

wee1-1 and *wee1-1 trd1-2* mutant root meristems grown in the absence and presence of HU. Only 25 genes were differentially regulated between *wee1-1* and *wee1-1 trd1-2* under control conditions (Supplemental Data Set 3), indicating that the *trd1* mutation induces only a limited transcriptional response. Moreover, all genes within a genomic region spanning *At2g38120* to *At2g38290* showed a uniform 2-fold induction, indicating a genome duplication, confirmed by whole-genome sequencing (Supplemental Figure 2). The transcriptional increase of the genes within this locus likely correlated with the increased gene copy number, rather than with RNase H2 deficiency, as no transcriptional induction was observed in the independent *wee1-1 trd1-1* mutant or in a *trd1-2* mutant in which the duplicated region was segregated from the mutation (Supplemental Figure 2). Among the seven remaining genes being transcriptionally upregulated, five appeared in a coexpression cluster (Supplemental Figure 3). The same genes were strongly activated in both genotypes after treatment for 24 h with HU (Supplemental Figure 4) and were differentially expressed between control plants and *trd1-2* mutants (Supplemental Figure 3). To pinpoint the underlying process that triggered the transcriptional response of these genes, we collected a list of genes being coexpressed with at least three of five genes present within the coexpression cluster (Supplemental Data Set 4), revealing an enrichment for DNA repair-related processes (Supplemental Data Set 5). In the presence of HU, none of the genes being differentially expressed between *wee1-1* and *wee1-1 trd1-2* displayed coexpression clusters or Gene Ontology enrichment (Supplemental Data Set 6).

As DNA repair commonly occurs through homologous recombination (HR), we introduced two different β-glucuronidase (GUS) recombination substrates (651 and IC9C) into the *trd1-2* mutant background. These recombination substrates contain an inactive *GUS* gene whose activity can be restored by either intra- and interchromosomal recombination in the 651 line or by interchromosomal recombination in IC9C (Swoboda et al., 1994; Molinier et al., 2004). Recombination frequencies can be deduced from the number of blue sectors after histochemical staining. When comparing plants grown with and without HU, an increase in recombination could be observed with both reporter lines in all genotypes tested, illustrating that HU treatment

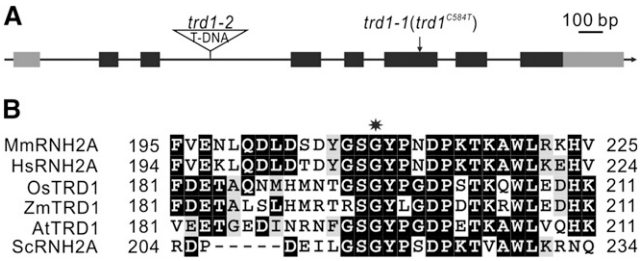

Figure 2. *TRD1* Encodes the Catalytic Subunit of the RNase H2 Complex.

(A) Intron-exon organization of *TRD1*. Black and gray boxes represent exons and untranslated regions, respectively. The position of the mutated base pair (*trd1-1*) and T-DNA insertion site (*trd1-2*) are indicated.
(B) Sequence alignment of the RNase H2 subunit A from different species highlighting the conserved position of the Gly residue (indicated by a star). Mm, *Mus musculus*; Hs, *Homo sapiens*; Os, *Oryza sativa*; Zm, *Zea mays*; At, *Arabidopsis thaliana*; Sc, *Saccharomyces cerevisiae*.

triggers HR (Figure 4). Remarkably, HR frequencies of *trd1-2* and *trd1-2 wee1-1* were already significantly increased (P value < 0.01) in comparison with the wild type and *wee1-1* in the absence of HU (2- to 4-fold in 651 line and 2- to 6-fold in IC9C line) (Figure 4), indicating that loss of *RNase H2* enhances HR in *Arabidopsis*. Adding HU to the medium stimulated HR but did not alter the overall trend among the lines, demonstrating an independence of the increased HR levels in the *RNase H2* knockout from the HU treatment.

Resolving Holliday junctions that arise during HR requires the MUS81 endonuclease (Mannuss et al., 2010). To test the impact of the increased HR in *RNase H2*-deficient plants, the *mus81-1* mutation was introduced into the *trd1-2* mutant. While the *trd1-2* and *mus81-1* mutants were phenotypically indistinguishable from control plants, double mutants showed a severe root and shoot growth inhibition phenotype (Supplemental Figure 5), demonstrating that HR resolution is essential for plant survival of *RNase H2*-deficient plants.

RNase H2 Subunit A Mutants Accumulate γ-H2AX Foci

HR is induced upon the occurrence of DSBs or replication fork destabilization that can be detected through immunodetection of γ-H2AX foci, representing a phosphorylated form of the histone variant H2AX (Kinner et al., 2008; Sirbu et al., 2011). To detect such genomic problems in the *RNase H2*-defective background, we performed in situ immunostaining experiments in wild-type, *wee1-1*, *trd1-2*, and *wee1-1 trd1-2 Arabidopsis* root tip nuclei, treated or untreated with HU, using a γ-H2AX antibody. As expected, no γ-H2AX foci were detected in mitotic root tip nuclei of untreated wild-type plants and *wee1-1* mutants. By contrast, upon HU treatment, nuclei of both genotypes displayed γ-H2AX foci (Figures 5A and 5B). Furthermore, the number of γ-H2AX foci per nucleus was significantly higher in the *WEE1*^{KO} background (Figure 5A). Surprisingly, *trd1-2* mutants showed a high number of γ-H2AX foci regardless of being HU treated or not (Figure 5B). Thus, in agreement with the transcriptomic analysis and the observed higher HR rates, plants lacking a functional RNase H2 complex accumulate chromosomal instability that can be visualized as γ-H2AX foci.

To analyze whether the DSBs in the *RNase H2* mutant could be the result of replication stress, we screened for a specific enrichment of γ-H2AX foci in replicating nuclei (Figure 5C). Root tips of *trd1-2* mutants were incubated for 1 h with the thymidine analog ethynyl deoxyuridine (EdU), labeling ~20% of all nuclei, representing the S- and early G2-phase nuclei that underwent replication during the EdU treatment. A total of 53% of all nuclei showed γ-H2AX foci and among these 86% scored Edu positive, illustrating a significant enrichment for replicating nuclei. These data clearly suggest that replication defects lay at the basis of the DSBs occurring in *RNase H2*-deficient plants.

Increased HR Does Not Rescue *WEE1*^{KO} HU Hypersensitivity

The observed increase of HR in *RNase H2* mutant plants might account for the suppression of the *WEE1* mutant phenotype in the presence of HU. To test this hypothesis, we suppressed HR in the

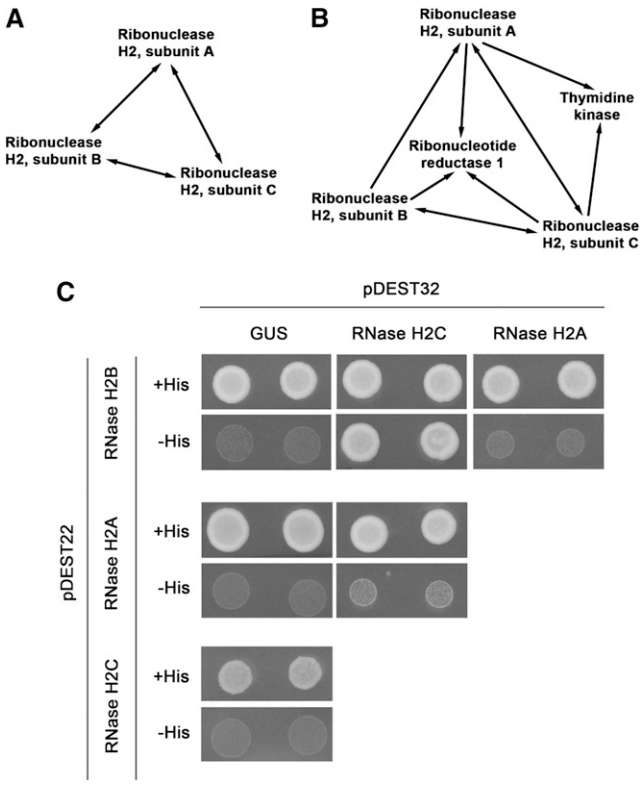

Figure 3. The *Arabidopsis* RNase H2 Complex Comprises Three Subunits.

(A) and **(B)** Protein-protein interaction between different RNase H2 subunits as identified by tandem affinity purification from cell cultures cultivated in the absence **(A)** or presence of 10 mM HU for 24 h **(B)**. Arrows point from bait to prey and correspond to interactions that were confirmed in a repeat experiment (Supplemental Data Set 2).
(C) Yeast two-hybrid interactions between the different subunits of RNase H2. The GUS protein was used as negative control.

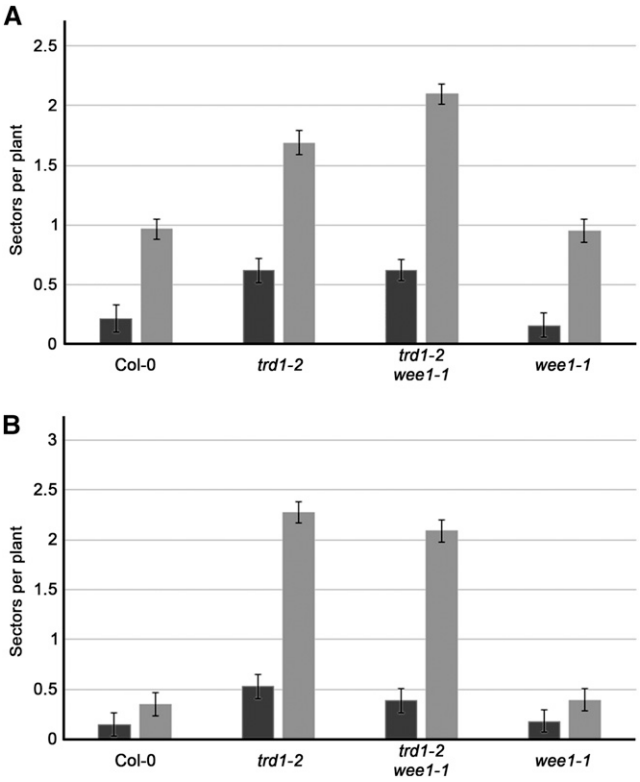

Figure 4. RNase H2 Deficiency Triggers Increased HR.

Recombination frequencies of untreated (black bars) and HU-treated (0.75 mM; gray bars) control (Col-0), *trd1-2*, *trd1-2 wee1-1*, and *wee1-1* seedlings using the 651 **(A)** or IC9C **(B)** reporters. Data represent mean number of GUS sectors ± SE (n = 4, minimum 50 plants per repeat).

double *trd1-2 wee1-1* mutant by introducing a mutant *XRCC2* allele, encoding an inactive RAD51 paralogous gene that causes hypersensitivity to the DNA cross-linking drug MMC (Bleuyard et al., 2005). Surprisingly, the *xrcc2-1* mutation did not remove the HU resistance phenotype of the *trd1-2 wee1-1* double mutants, but instead enhanced it, conferring root growth on HU-supplemented medium that was equal to that of control plants (Supplemental Figure 6). Similarly, *xrcc2-1* partially rescued the HU hypersensitive phenotype of the single *wee1-1* mutants (Figures 6A to 6C). Similar data were obtained using a mutation in the paralogous *RAD51C* gene (Figures 6D to 6F). Thus, HR contributes to the HU sensitivity of the *wee1-1* lines, rather than rescuing it.

RNase H2 Deficient Plants Incorporate rNMPs into Their Genome

Yeast and mouse genomes defective in *RNase H2* activity incorporate rNMPs (Nick McElhinny et al., 2010a; Miyabe et al., 2011; Reijns et al., 2012). Because rNMPs possess a reactive 2'OH on the sugar part, their incorporation makes the DNA backbone more susceptible to strand cleavage by alkali. Therefore, incubating genomic DNA in KOH and subsequently monitoring the resulting fragmentation by alkaline agarose gel electrophoresis can detect the presence of ribonucleotides in DNA. We analyzed the level of rNMP incorporation in the genomic DNA of wild-type, *wee1-1*, *trd1-2*, and *trd1-2 wee1-1* plants grown under control conditions or in the presence of HU. Under both conditions, the genomic DNA samples isolated from *trd1-2* and *trd1-2 wee1-1* mutants were more sensitive to alkaline hydrolysis than DNA samples isolated from the wild type and *wee1-1*, as observed by the accumulation of short DNA fragments (Figure 7). No strong effect of HU application on the DNA fragmentation was observed, indicating that the absence of RNase H2 activity is the main cause of DNA instability. Similar as observed for *trd1-2*, DNA fragmentation indicative of rNMP incorporation was detected for DNA isolated from RNase H2 subunit B or subunit C mutant plants (Supplemental Figure 7).

Lack of RNase H2 Activity Results in an Increased Mutation Rate

Root growth analysis of the *RNase H2*-deficient plants suggested that these plants appear to suffer no growth penalties for substituting dNTPs for rNTPs. However, short-term growth analyses do not exclude genomic defects over the long term. Therefore, we sequenced and compared the genome of a single wild-type, *wee1-1*, *trd1-2*, and *trd1-2 wee1-1* plants, grown side-by-side over three generations. The sequence reads were mapped to the *Arabidopsis* reference genome (TAIR10) and scored for base pair changes and short base pair deletions. The number of base substitutions was not significantly different among the different genotypes (Table 1). By contrast, whereas both wild-type and *wee1-1* plants showed no base pair deletions, *trd1-2* and *trd1-2 wee1-1* displayed three and two 2-bp deletions, respectively. Additionally, the *trd1-2* mutant showed a 3-bp deletion (Table 1). Sequencing of the mutant loci over different generations confirmed the presence of the small deletions and illustrated that all but the 3-bp deletion were generated within less than two generations (Figure 8).

A parallel genome sequencing experiment was conducted on plants grown in the constant presence of HU. Again, plants lacking RNase H2 activity (*trd1-2* and *trd1-2 wee1-1*) did accumulate small base pair deletions that were demonstrated by direct sequencing to be absent in the grandparent lines (Supplemental Data Set 7 and Supplemental Figure 8). By contrast, no deletions were found in the RNase H2 proficient plants (wild type and *wee1-1*). Compared with the control-grown plants, the HU treatment appeared to have no effect on the number of deletions. Indeed, linear regression analysis showed that only the presence of the *trd1-2* mutation correlated with the total number of deletions (estimated coefficient of 2.36, P value < 0.001). Thus, absence of RNase H2 appeared to trigger genome instability in the form of small deletions.

DISCUSSION

The *Arabidopsis WEE1* gene is essential for growth adaptation under replication stress, both from exogenous or endogenous origin (De Schutter et al., 2007; Takahashi et al., 2008). Here, we show that deficiency in RNase H2 activity reverts the replication stress hypersensitivity of *WEE1^{KO}* mutants and delimits the cell

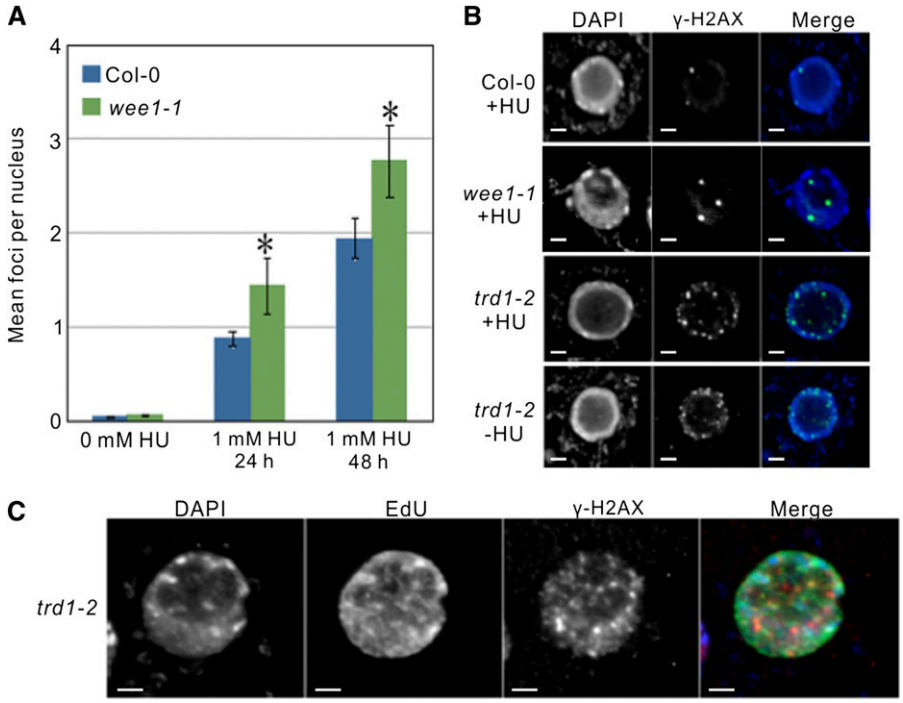

Figure 5. Lack of RNase H2 Activity Triggers the Accumulation of γ-H2AX Foci.

(A) Average number of γ-H2AX foci per nucleus of wild-type (Col-0) and *wee1-1* mutants, untreated or treated with HU. Data represent mean ± SD (n = 100, *P value < 0.05, two-sided Student's t test).

(B) Detection of γ-H2AX foci in wild-type (Col-0), *wee1-1*, *trd1-2*, and *wee1-1 trd1-2* root tip cells untreated (−HU) or treated with 1 mM HU (+HU). Bar = 2 μm.

(C) γ-H2AX immunofluorescence in S- or early G2-phase nuclei of *trd1-2* mutants (being Edu positive). Bar = 2 μm.

death phenotype that is caused by premature vascular cell differentiation. *WEE1*-deficient plants display a smaller root meristem upon replication stress, which is due to a reduction in the number of proliferating cells, resulting in a short root phenotype. We previously demonstrated that a prolonged S-phase underlies this growth phenotype (Cools et al., 2011). Absence of RNase H2A reverts the short root phenotype by restoring meristem size, implying that mutation of the *RNase H2* gene restores the replication rate of the *WEE1* knockouts.

The TAP experiment revealed that the RNase H2 complex of *Arabidopsis* comprises three subunits that are homologs of the mammalian and yeast catalytic and regulatory subunits, confirming their importance during evolution. An intriguing observation in the TAP experiment is the pull-down of thymidine kinase and the large subunit of ribonucleotide reductase 1 (RNR1) in the presence of HU. Thymidine kinase supplies an important precursor, deoxythymidine monophosphate, for nucleic acid biosynthesis. RNR catalyzes the formation of dNTPs from rNTPs. As HU limits the available sources of dNTPs for DNA synthesis, it is possible that the association of thymidine kinase and RNR with the RNase H2 complex represents a mechanism to obtain a local enrichment of dNTPs to be used to replace the excised rNTPs.

In contrast to mouse and yeast, knockout of RNase H2 in plants does not result in a slow growth phenotype (Nick McElhinny et al., 2010a; Hiller et al., 2012; Reijns et al., 2012) that has been attributed to the activation of a DNA damage checkpoint, as visualized by the accumulation of γ-H2AX foci. Such foci are also observed in the *Arabidopsis RNase H2* mutant plants. The lack of growth arrest in *Arabidopsis* indicates that the plant DNA damage checkpoints might be less robust or repair more efficiently. Alternatively, the impact of rNMP incorporation in non-plant species might be higher, which would correspond with the limited effect of RNase H2 deficiency on the *Arabidopsis* transcriptome, whereas the equivalent knockout in yeast results in changes in expression of hundreds of genes (Arana et al., 2012). The few genes being activated in the *trd1* mutant appear in a coexpression cluster functionally linked to DNA repair. Correspondingly, an increased HR rate was observed in the *trd1-2* background. These results are consistent with observations in yeast in which lack of RNase H2 activity increases the recombination frequency (li et al., 2011). Given the accumulation of γ-H2AX foci in S-phase nuclei, single-strand breaks encountered by the replication fork could be converted into DSBs during DNA synthesis. The phenotype of the *trd1-2 mus81-1* double mutant supports such a need for increased HR to deal with rNMP incorporation. MUS81 is a conserved endonuclease involved in the resolution of Holliday-like DNA junctions (Mannuss et al., 2010), and the synthetic lethality of *trd1* with *mus81* indicates that MUS81 is required to resolve the

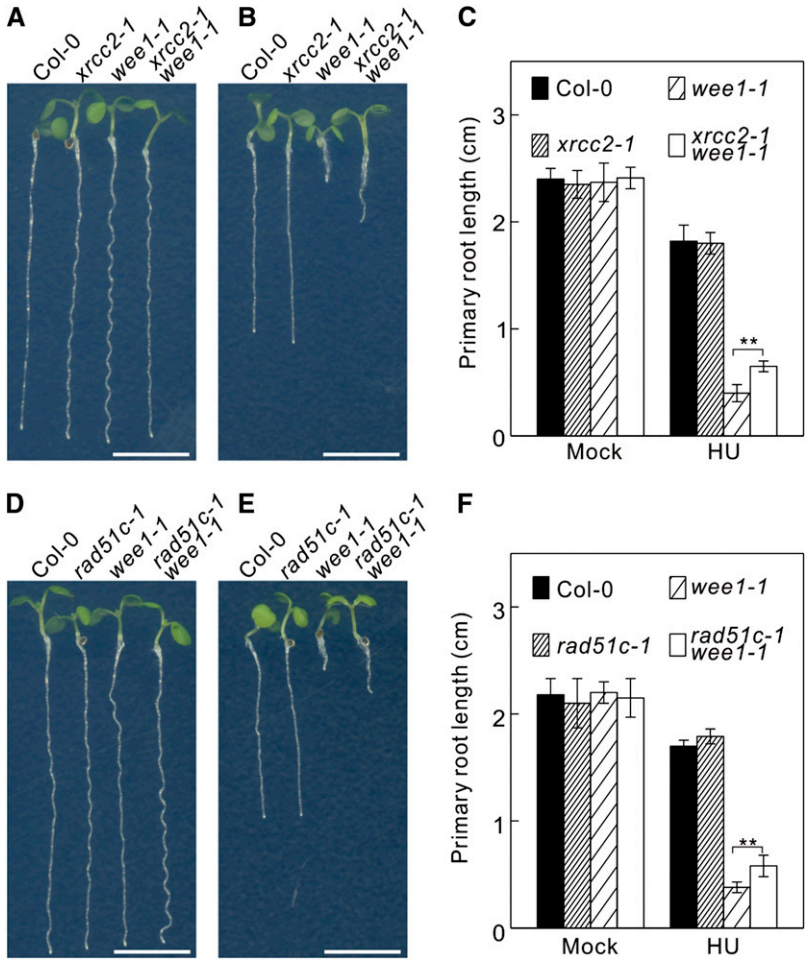

Figure 6. Mutations in *XRCC2* and *RAD51C* Partially Rescue *WEE1*^{KO} HU Hypersensitivity.

(A) and **(B)** Root growth of 7-d-old wild-type (Col-0) and *xrcc2-1*, *wee1-1*, and *xrcc2-1 wee1-1* mutant plants grown on control medium **(A)** or medium supplemented with 0.75 mM HU **(B)**. Bar = 0.5 cm.

(C) Quantification of the root length of plants shown in **(A)** and **(B)**. Data represent mean ± SD ($n > 10$, **P value < 0.01, two-sided Student's *t* test).

(D) and **(E)** Root growth of 7-d-old wild-type (Col-0) and *rad51c-1*, *wee1-1*, and *rad51c-1 wee1-1* mutant plants grown on control medium **(D)** or medium supplemented with 0.75 mM HU **(E)**. Bar = 0.5 cm.

(F) Quantification of the root length of plants shown in **(D)** and **(E)**. Data represent mean ± SD ($n > 10$, **P value < 0.01, two-sided Student's *t* test).

[See online article for color version of this figure.]

resulting replication intermediates arising in the absence of RNase H2.

The increased HR rate caused by absence of RNase H2 activity cannot account for the observed rescue of the *wee1-1* phenotype. Contrary, triple mutant *trd1-2 wee1-1 xrcc2-1* plants displayed a stronger recovery phenotype than that seen in *trd1-2 wee1-1* under replication stress (Supplemental Figure 6). Similarly, *wee1-1 xrcc2-1* and *wee1-1 rad51c-1* double mutants tolerated HU better than the single *wee1-1* mutant. Possibly, unwinding of double-stranded DNA at a stalled replication fork in the absence of replication results in artificial HR substrates that trigger inaccurate recombinational repair, similar as postulated for plants deficient in DNA polymerase δ activity (Schuermann et al., 2009). Therefore, it is tempting to speculate that amelioration of the *wee1-1* and *trd1-2 wee1-1* phenotype in the absence of XRCC2 or RAD51C might be due to a decrease in the level of toxic genome rearrangements induced by HR. This suggests that one of the roles of WEE1 upon replication stress is to coordinate replication fork unwinding with replication fork progression. In yeast and mammals, this is accomplished by reducing the activity of the S-phase CDKs through action of the ATR-CHK1 pathway that inhibits CDC25 (Cook, 2009; Willis and Rhind, 2009; Zegerman and Diffley, 2009). Since in plants the CDC25 phosphatase is not present and its antagonist WEE1 has a prominent role in the S-phase (Boudolf et al., 2006; Cools et al., 2011), it is very likely that in plants the inhibition of CDKs during a compromised S-phase is executed by an activation of WEE1. The resulting decrease in CDK activity might help in

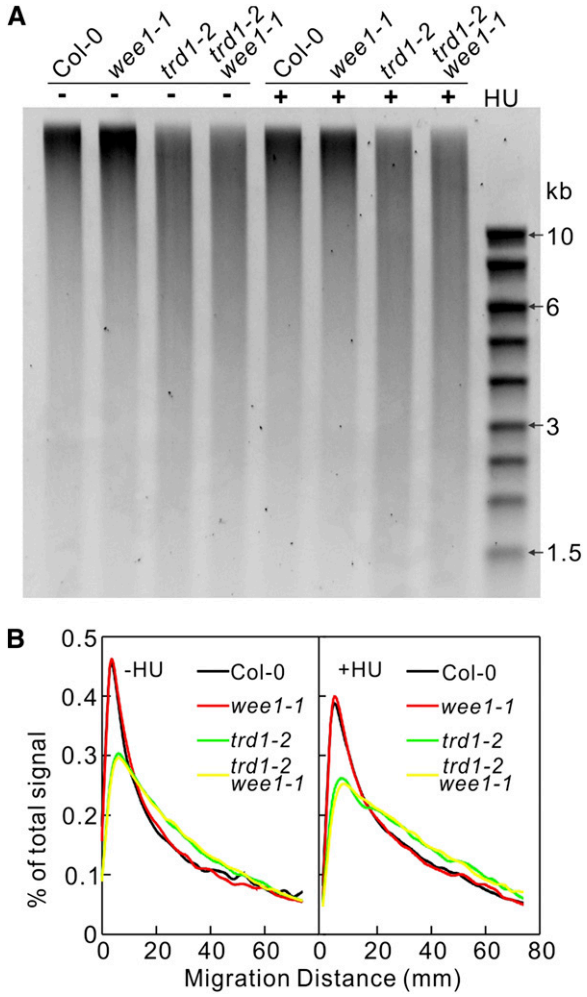

Figure 7. RNase H2-Deficient Plants Accumulate rNMPs in DNA.

(A) Alkaline cleavage products of genomic DNA extracted from 7-d-old wild-type (Col-0), *wee1-1*, *trd1-2*, and *trd1-2 wee1-1* seedlings grown under control conditions or in the presence of 0.75 mM HU.
(B) Densitometry plot of lanes in **(A)**.

adjusting the replication pace to the depletion of dNTPs triggered by the treatment with HU. The inability to control the activity of the replication forks probably results in the generation of long strands of ssDNA, as DNA replication halts but unwinding continues, eventually resulting in inappropriate HR substrates (Lopes et al., 2001; Sogo et al., 2002; Branzei and Foiani, 2010). These data are substantiated by the observed increase in the number of γ-H2AX foci in *WEE1*^{KO} plants in the presence of HU.

If the increased HR rate of the *trd1-2* mutants does not account for the rescue of the HU sensitivity of the *wee1-1* plants, what does? One possible explanation might be that in wild-type plants, RNase H2-dependent repair, triggered by the incorporation of rNMPs in DNA, might generate some type of DNA structure that induces a WEE1-dependent checkpoint. In this scenario in the absence of RNase H2, these aberrant DNA structures might not occur, reducing the need for the WEE1 kinase. However, this hypothesis appears unlikely, given that wild-type and *RNase H2*-deficient plants do not display a differential level of *WEE1* expression. Moreover, both in the absence and presence HU, no difference in meristem size between wild-type and *trd1-2* mutant plants is observed (Supplemental Figure 9), indicating the lack of an RNase H2-dependent cell cycle checkpoint. Rather, we postulate that the ability to tolerate substitution of dNTPs with rNTPs in the *RNase H2*-deficient mutant facilitates fork progression at a normal pace in *WEE1*^{KO} plants, thereby limiting the above-mentioned ssDNA that would be prone to produce toxic structures through recombination. Alternatively, unwounded ssDNA on the lagging strand might be stabilized by the continuous presence of RNA primers of Okazaki fragments or hybrids between transcripts and DNA. Incorporating rNMP into the DNA, however, results in a fragile genome, as the reactive 2'-hydroxyl on the ribose ring sensitizes the DNA backbone to cleavage. In budding yeast, rNMP incorporation in the absence of RNase H2 causes the accumulation of 2- to 5-bp deletions within short tandem repeats, which is largely dependent on topoisomerase 1 (TOP1) activity (Nick McElhinny et al., 2010a; Kim et al., 2011; Williams et al., 2013). In general, TOP1 mediates the removal of replication- and transcription-associated supercoils (Wang, 2002). In addition to this function, TOP1 acts as an endonuclease at RNA-DNA junctions (Sekiguchi and Shuman, 1997). Ligation of the generated ends within short directed repeats might cause misalignment of the complementary strands, resulting in the loss of one repeat unit following replication (Williams and Kunkel, 2014). Similarly, we found that over less than three generations, plants lacking a functional RNase H2 complex accumulated slippage mutations, mostly in simple base pair repeats, whereas the number of base substitutions was not affected. The number of small deletions did not increase when plants were grown in the continuous presence of HU, suggesting that the number of rNMPs incorporated is mainly determined by the absence of RNase H2 activity, supported by the observation that the DNA fragmentation pattern was not more pronounced in the HU-treated samples (Figure 7). Interestingly, a large genome duplication was found in the *trd1-2* mutant. Although at this stage it cannot be excluded that this duplication might originate from an event independent of the absence of RNase H2 activity, large chromosomal rearrangements have also been observed in RNase H2-defective mouse embryonic fibroblasts (Reijns et al., 2012). These rearrangements have been speculated to result from DNA breaks due to unrepaired rNMPs in DNA (Williams and Kunkel, 2014). Thus, although RNase H2 deficiency allows overcoming a shortage in dNTPs, it increases genome instability and would be expected to affect fitness of the organism over multiple generations.

Table 1. Number of Base Substitutions and Deletions in Control (Col-0), *wee1-1*, *trd1-2*, and *trd1-2 wee1-1* Plants Compared to the Reference Genome (TAIR10)

Genotype	Base Substitution	1 bp Δ	2 bp Δ	3 bp Δ
Col-0	9	0	0	0
wee1-1	6	0	0	0
trd1-2	8	0	3	1
trd1-2 wee1-1	9	1	2	0

Sequence read	Genotype	Chromsome position	Deletion length(bp)
No. 1	*trd1-2*	Chr1_27943292-27943293	2
No. 2	*trd1-2*	Chr3_22692908-22692909	2
No. 3	*trd1-2*	Chr5_9404578-9404579	2
No. 4	*trd1-2wee1-1*	Chr3_12730324	1
No. 5	*trd1-2wee1-1*	Chr4_290002-290003	2
No. 6	*trd1-2wee1-1*	Chr4_2760416-2760417	2

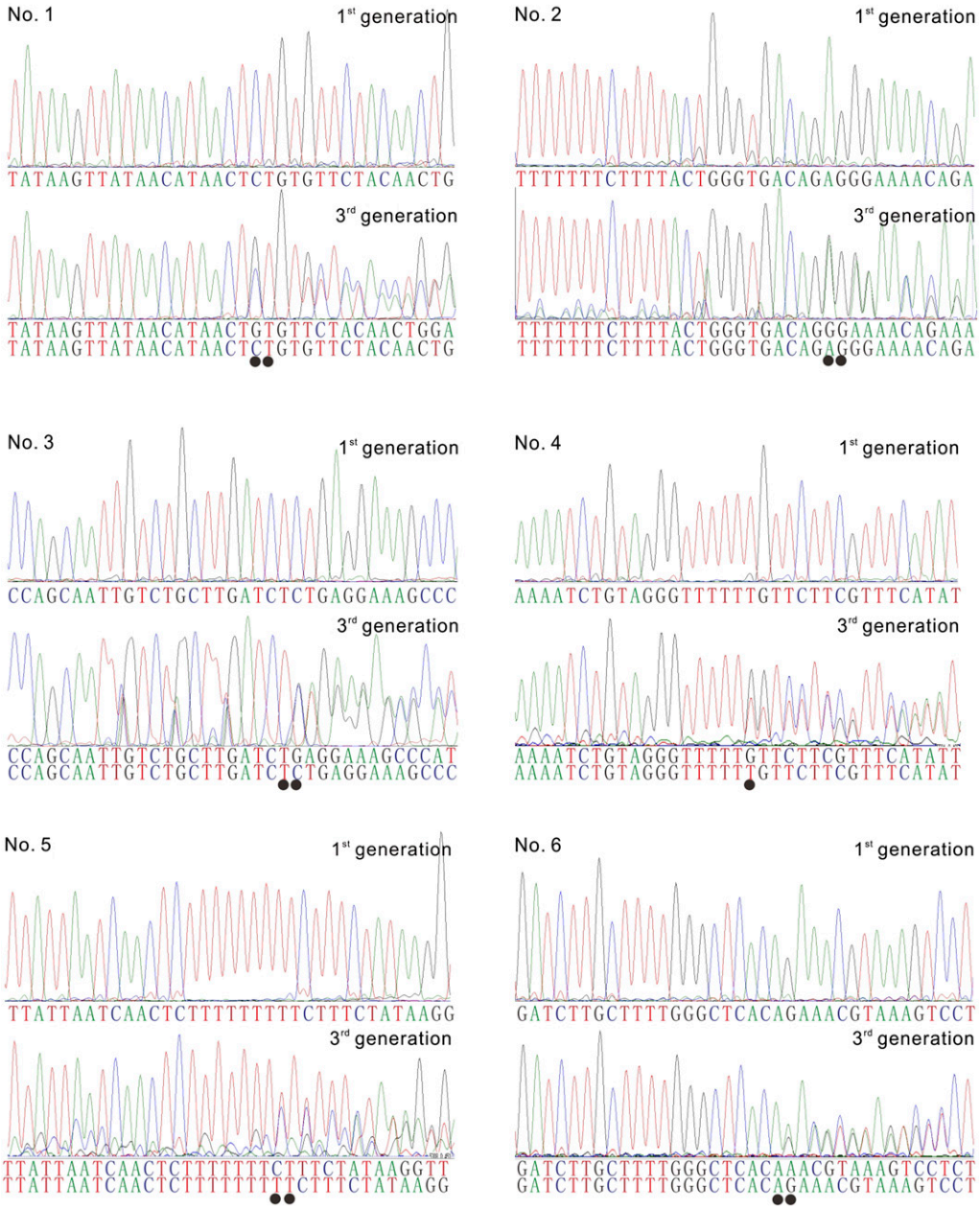

Figure 8. Lack of RNase H2 Activity Causes Small Base Pair Deletions.

Sequencing reads of mutant loci in first versus third generation plants. Deleted base pairs (indicated by dots) result in dual sequence reads.

METHODS

Plant Materials and Growth Conditions

Arabidopsis thaliana plants were grown in vitro vertically under long-day conditions (16 h light/8 h darkness) at 21°C on half-strength Murashige and Skoog medium (2.151 g/L) (Duchefa), 10 g/L sucrose, and 0.5 g/L MES, pH 5.7, adjusted with 1 M KOH and 10 g/L agar. For drug treatments, the HU concentration used was 0.75 mM for direct germination and 1 mM for transfer experiments. The *wee1-1*, *rad51c-1*, *xrcc2-1*, and *mus81-1* lines have been described previously (Bleuyard et al., 2005; De Schutter et al., 2007; Hartung et al., 2007). The *trd1-2* allele (GABI-139H04) was obtained from the GABI-Kat T-DNA mutant collection (Li et al., 2003), whereas the *rnh2b-1* (SAIL_609_A02) and *rnh2c-1* (SALK_043851) alleles were obtained from the Salk Institute T-DNA Express database. Genotyping primers are listed in Supplemental Data Set 9.

Ethyl Methanesulfonate Mutagenesis and Mapping

WEE1^{KO} mutant seeds were soaked for 12 h in 0.25% (v/v) ethyl methanesulfonate (Sigma-Aldrich) and then washed two times for 15 min with 0.1 M sodium thiosulfate (Sigma-Aldrich) and two times for 15 min with water, dried, and sown in 200 pools of each 250 seeds. After self-fertilization of the M0, the M1 seeds were grown, and the M2 seeds were collected from individual M1 plants. The M2 plants were screened for restoration of root growth on vertical plates containing HU.

Leaf samples of *wee1-1 trd1-1* plants were used for nuclear DNA extraction according to Schneeberger et al. (2009). The leaves were bulked prior to DNA extraction. Illumina True-Seq libraries were generated from extracted DNA according to the manufacturer's protocol and sequenced on an Illumina HiSeq2000 50-bp single read run. The SHORE pipeline (Ossowski et al., 2008) was used for the alignment to the reference genome (Col-0; TAIR8). Base counts per position and single nucleotide polymorphisms are also determined based on the alignments. The candidate zone is narrowed based on the relative allele frequencies of the two parents (Col-0 and Landsberg *erecta*) by SHOREmap (Schneeberger et al., 2009).

Confocal Microscopy and Root Growth Measurements

To visualize meristems, root tips were stained for 2 min in a 10 μM propidium iodide solution (Sigma-Aldrich) and were analyzed with either an LSM 510 or LSM 5 exciter confocal microscope (Zeiss). For root growth measurements, the position of the root tips was marked daily on the plate and length of the roots was measured and analyzed by ImageJ.

Tandem Affinity Purification and Liquid Chromatography-Tandem Mass Spectrometry Analysis

Cloning of transgenes encoding tag fusions under control of the constitutive cauliflower mosaic virus 35S promoter and transformation of *Arabidopsis* cell suspension cultures were performed as previously described (Van Leene et al., 2007). Tandem affinity purification of protein complexes was done using the GS tag (Van Leene et al., 2008) followed by a downscaled purification protocol and liquid chromatography-tandem mass spectrometry analysis on LTQ Orbitrap Velos (Thermo Fisher Scientific) as described by Cuéllar Pérez et al. (2014). A list of nonspecific background proteins was assembled by combining our previous background list (Van Leene et al., 2010) with background proteins from control GS purifications on mock, GFP-GS, and GUS-GS cell culture extracts identified with LTQ Orbitrap Velos. To obtain the final list of interactors, these background proteins were subtracted from the list of identified proteins.

Yeast Two-Hybrid Analysis

Plasmids encoding the bait (pDEST32) and prey (pDEST22) were transformed into the yeast strain PJ69-4α (MATα; trp1-901, leu2-3,112, ura3-52, his3-200, gal4Δ, gal80Δ, LYS2::GAL1-HIS3, GAL2-ADE2, met2GAL7-lacZ) and PJ69-4a (MATa; trp1-901, leu2-3,112, ura3-52, his3-200, gal4Δ, gal80Δ, LYS2TGAL1-HIS3, GAL2-ADE2, met2TGAL7-lacZ) by the LiAc method (Gietz et al., 1992). Transformed yeast cells were selected on synthetic dextrose plates without Leu (pDEST 32) or without Trp (pDEST22). Interactions between proteins were assayed by the mating method (Bendixen et al., 1994).

RNA Sequencing

The *WEE1* knockout (*wee1-1*) and the *RNH2A/WEE1* double knockout (*trd1-2 wee1-1*) seeds were germinated on control medium on a nylon mesh and transferred 5 d after germination to control medium or medium supplemented with 2 mM HU. Each sample had three independent biological repeats. Twenty-four hours after the transfer, 200 root tips (<2 to 3 mm) were collected and frozen in liquid nitrogen. RNA was extracted from root tissue with the RNeasy Plant Kit (Qiagen). Illumina True-Seq libraries were generated from cDNA according to the manufacturer's protocol and sequenced on a HiSeq2000. Quality of the reads (Phred quality score) was calculated by FASTQC from Babraham Bioinformatics. After filtering and trimming using a FASTX toolkit (by Assaf Gordon at Cold Spring Harbor Laboratory), reads were aligned to the *Arabidopsis* genome (TAIR10) using Genomic Short-read Nucleotide Alignment Program (Wu and Nacu, 2010). Tables of counts were produced using the Python software htseq-counts. Afterwards, empirical analysis of gene expression data was calculated and normalized in R environment using edgeR from Bioconductor.

Quantitative RT-PCR

RNA was extracted from root tip tissue with the RNeasy plant kit (Qiagen), and cDNA was prepared from 500 ng of total RNA with the iScript cDNA synthesis kit (Bio-Rad) according to the manufacturer's instructions. Quantitative RT-PCR was performed with LightCycler 480 SYBR Green I Master (Roche) in a final volume of 5 μL and 0.2 mM primer concentration and analyzed with a LightCycler 480 (Roche). For each reaction, three technical repeats and two to three biological repeats were done. The primer sequences were 5′-CTCTCGTTCCAGAGCTCGCAAAA-3′ and 5′-AAGAACACGCATCCTACGCATCC-3′ for *EMB2386* (AT1G02780), 5′-CCGTACCGGGAAAGATAACGAAGA-3′ and 5′-CACTTGAGCCACTTGGTTAGATGC-3′ for AT2G38120, 5′-GGTTTGCCTTGAAGGTTCTTCACC-3′ and 5′-CCATGACCTGAAGGATGAGGATGA-3′ for AT2G38180, 5′-CTTCTCTTCCAGATGCCACTCCTT-3′ and 5′-AAGCTCTCCCTTCAGATGGCGTAT-3′ for AT2G38280, 5′-TGTTTAAATCGCTGCCCAACCTGG-3′ and 5′-CAAAATGCGGGTGGAAGAAGTCATC-3′ for AT5G60250, 5′-TGTACCCCCACGAAGCTCCTAA-3′ and 5′-TGCAGCTGCTTCATGGTTCAGAG-3′ for AT2G18600, 5′-TCCCAAAGGCGGTAAGGCAAAC-3′ and 5′-GTCCGATCACCGCGAGGTATTT-3′ for *NAC103* (AT5G64060), 5′-TCCCTCGATTCGCTTCTGGATG-3′ and 5′-AGTCAACCCCGCAACAACGAGA-3′ for *TRFL10* (AT5G03780), 5′-ATGGCGTTCTGCTCCTCTGC-3′ and 5′-GGTGCTGTTTTCCCCACACC-3′ for *PARP2* (AT4G02390), 5′-TCTCTTTGCAGGATGGGACAAGC-3′ and 5′-AGACTGAGCCGCCTGATTGTTTG-3′ for *PAC1* (AT3G22110), and 5′-GACTTTCAAGCGCAGGAATGGTG-3′ and 5′-CCTTGTCCTTGGGGCAACACTTT-3′ for *RPS26C* (AT3G56340). *EMB2386*, *PAC1*, and *RPS26C* were used as reference genes. Statistical analysis was executed with the Statistical Analysis Software (SAS Enterprise Guide 5.1; SAS Institute) using the mixed model procedure, and P values were Bonferroni adjusted for multiple measurements.

Homologous Recombination Assay

Two recombination substrates, 651 (Swoboda et al., 1994) and IC9C (Molinier et al., 2004), were crossed to *trd1-2 wee1*, *trd1-2*, *wee1-1*, and Col-0. For the HR recombination assay, 50 seeds of each line were germinated on half-strength Murashige and Skoog medium with or without 0.75 mM HU. The restoration of the reporter gene was visualized by histochemical GUS staining according to the standard protocol (Jefferson et al., 1987). HR events of individual plants were assessed visually using a binocular microscope. The HR assays were repeated three times, and the mean values were calculated. Statistical analysis was executed with the Statistical Analysis Software (SAS Enterprise Guide 5.1) using the mixed model procedure, and P values were Bonferroni adjusted for multiple measurements.

Detection of Alkali-Sensitive Sites in Genomic DNA

Genomic DNA was isolated using a DNeasy plant kit (Qiagen). Either KOH or KCl was added to genomic DNA to a final concentration of 0.3 M in 40 μL volumes and incubated at 55°C for 2 h. Following treatment, 6× alkaline loading buffer (300 mM KOH, 6 mM EDTA, 18% Ficoll [Type 400], 0.15% bromocresol green, and 0.25% xylene cyanol) was added to KOH-treated samples. Neutral loading buffer (30% glycerol in TE buffer, 0.25% bromophenol blue, and 0.25% xylene cyanol) was added to KCl-treated samples. Electrophoresis of alkaline-treated samples was performed using a 50 mM NaOH, 1 mM EDTA, and 1% agarose alkaline gel with 50 mM NaOH, 1 mM EDTA electrophoresis buffer (Sambrook et al., 2006). Electrophoresis of KCl-treated samples was performed using a 1% agarose gel and TBE buffer. Electrophoresis of the samples was at 1 V/cm for 18 h. Alkaline gels were neutralized by soaking in 1 M Tris HCl, pH 8.0, and 1.5 M NaCl for 1 h and then stained with SYBR Gold (Invitrogen). Signal intensity per lane was measured with ImageJ and normalized to the total signal intensity per lane. Data were smoothed using a LOESS (Local Regression) algorithm.

Immunostaining Using γ-H2AX Antibodies

Slide preparation, immunostaining, quantification of γ-H2AX foci of mitotic nuclei, and EdU staining were performed as previously described (Amiard et al., 2010).

Whole-Genome Sequencing

Col-0, *wee1-1*, *trd1-2*, and *trd1-2 wee1-1* plants were grown side-by-side using the Araponics system (http://www.araponics.com) for three generations, either in the absence or continuous presence of 0.75 mM HU. Medium was renewed once a week. We sequenced two genomes for each genotype: one from a plant grown under control conditions and one from a plant grown in the presence of HU (eight genomes in total). Genomic DNA was extracted using a DNeasy plant kit (Qiagen). Paired-end Illumina True-Seq libraries were generated from extracted DNA according to the manufacturer's protocol and sequenced in multiplexes of four on a HiSeq2000 leading to an average coverage between 43 and 47× per sample. Each genome was sequenced to nearly the same genome-wide sequencing coverage (Supplemental Data Set 10). To estimate the sequencing error rate in each sample, we followed the approach described by Ossowski et al. (2008). Briefly, we used sites covered by at least 10 and <70 reads, in which the consensus base was the same in all eight genomes sequenced, and no more than 20% of reads call a discordant base in any of the sequenced genomes. We subsampled five times 1% of the sites in each genome and estimated error frequencies. We found that error rates were very similar across replicates, indicating no positional bias. Estimated error frequencies were also very similar across genomes. The average error frequency was 0.08% and ranged from 0.076 to 0.086% (Supplemental Data Set 10). The sequencing errors identified showed the same base pair spectrum in all sequenced genomes (paired Mann-Whitney U Test, P value > 0.05). Moreover, there was no indication that single base pair deletions have a higher probability to be erroneously called in any of the genomes, also not when comparing the classes of genomes with TRD1 and without (Mann-Whitney U Test, P value > 0.05). Therefore, the detection of an increased number of mutations in one genome is most likely not due to an increased sequencing error rate for this genome.

To identify newly induced single base pair substitutions, we followed the consensus approach described by Ossowski et al. (2008). Base changes were called if one of the sequenced genomes differed from all others (control genomes). We excluded sites suspected to be noise sources, like repetitive regions. Each site had to be covered by at least five reads in every genome. No control genome was allowed to contain erroneous reads, defined as a subset of reads that report a base different from the majority. If more than one base was reported for one site, the variant base had to be supported by 20% of the reads but at least three reads. Between 88.1 and 88.2 million sites matched those quality criteria in each sequenced genome reflecting a similar sequencing quality. The dependency of the number of genomic deletions on the different mutations (*wee1-1* and *trd1-2*) and treatments (−HU and +HU) was statistically analyzed by applying linear regression on log-transformed count data.

Accession Numbers

RNA sequencing data have been submitted to ArrayExpress (www.ebi.ac.uk/arrayexpress) under accession number E-MTAB-2590. Sequence data from this article can be found in the Arabidopsis Genome Initiative or GenBank/EMBL databases under the following accession numbers: *WEE1* (At1g02970), *TRD1/RNH2A* (At2g25100), *RNH2B* (At4g20325), *RNH2C* (At2g39440), *RAD51C* (At2g45280), *XRCC2* (At5g64520), *MUS81* (At4g30870), *MmRNH2A* (NP_081463), *HsRNH2A* (NP_006388), *OsTRD1* (NP_001065783), *ZmTRD1* (NP_001152248), and *ScRNH2A* (NP_014327).

Supplemental Data

The following materials are available in the online version of this article.

Supplemental Figure 1. Mutations in the Regulatory Subunits of the RNase H2 Complex Partially Rescue the HU Hypersensitivity Phenotype of *WEE1^{KO}* Plants.

Supplemental Figure 2. The *trd1-2* Mutant Holds a Large DNA Duplication.

Supplemental Figure 3. Absence of RNase H2 Activates a DNA Repair Coexpression Cluster.

Supplemental Figure 4. Transcriptional Induction of *trd1-2* Differentially Expressed Genes by HU.

Supplemental Figure 5. The *trd1-2* Mutant Is Synthetically Lethal in a *mus81* Mutant Background.

Supplemental Figure 6. Simultaneous Knockout of *XRCC2* and *TRD1* Rescues the HU Hypersensitivity Phenotype of *WEE1^{KO}* Plants Completely.

Supplemental Figure 7. *RNase H2* Mutant Plants Accumulate rNMPs in DNA.

Supplemental Figure 8. Confirmation of Small Base Pair Deletions in *RNase H2*-Deficient Plants Grown in the Presence of HU.

Supplemental Figure 9. Number of Meristematic Cortex Cells in Wild-Type (Col-0) and *trd1-2* Mutant Roots.

Supplemental Data Set 1. Protein Identification Details Obtained with the LTQ Orbitrap Velos (Thermo Fisher Scientific) and Mascot Distiller

Software (Version 2.4.1; Matrix Science) Combined with the Mascot Search Engine (Version 2.3; Matrix Science) and Database TAIR10.

Supplemental Data Set 2. Proteins Identified in TAP Experiments with as Baits Ribonuclease H2, Subunits A, B, and C, Either without and with HU Treatment.

Supplemental Data Set 3. Differentially Expressed Genes in *trd1-2 wee1-1* versus *wee1-1* Root Tips under Control Conditions.

Supplemental Data Set 4. Genes Coexpressed with at Least Three Genes Induced in *trd1-2* Mutants.

Supplemental Data Set 5. GO Enrichment of Coexpressed Genes.

Supplemental Data Set 6. Differentially Expressed Genes in *trd1-2 wee1-1* versus *wee1-1* Root Tips upon HU Treatment.

Supplemental Data Set 7. Number of Base Substitutions and Deletions in HU-Treated Control (Col-0), *wee1-1*, *trd1-2*, and *trd1-2 wee1-1* Plants.

Supplemental Data Set 8. Statistical Analysis of the Variables Linked to Genome Deletions.

Supplemental Data Set 9. List of Primers Used for Genotyping.

Supplemental Data Set 10. Sequencing Summary.

ACKNOWLEDGMENTS

We thank Annick Bleys for help in preparing the article. This work was supported by grants from the Research Foundation Flanders (G.0C72.14N) and the Interuniversity Attraction Poles Programme (IUAP P7/29 "MARS"), initiated by the Belgian Science Policy Office. T.C. is a Postdoctoral Fellow of the Research Foundation-Flanders.

AUTHOR CONTRIBUTIONS

P.K., Z.H., G.D.J., K.S., C.I.W., and L.D.V. conceived and designed the research. P.K., Z.H., T.C., S.A., N.D.W., and E.-M.W. performed the experiments. P.K., Z.H., T.C., S.A., E.-M.W., G.D.J., K.G., K.S., C.I.W., and L.D.V. analyzed the data and wrote the article. All authors read, revised, and approved the article.

Received May 26, 2014; revised August 10, 2014; accepted August 29, 2014; published September 12, 2014.

REFERENCES

Amiard, S., Charbonnel, C., Allain, E., Depeiges, A., White, C.I., and Gallego, M.E. (2010). Distinct roles of the ATR kinase and the Mre11-Rad50-Nbs1 complex in the maintenance of chromosomal stability in Arabidopsis. Plant Cell **22:** 3020–3033.

Arana, M.E., Kerns, R.T., Wharey, L., Gerrish, K.E., Bushel, P.R., and Kunkel, T.A. (2012). Transcriptional responses to loss of RNase H2 in *Saccharomyces cerevisiae*. DNA Repair (Amst.) **11:** 933–941.

Bendixen, C., Gangloff, S., and Rothstein, R. (1994). A yeast mating-selection scheme for detection of protein-protein interactions. Nucleic Acids Res. **22:** 1778–1779.

Bleuyard, J.Y., Gallego, M.E., Savigny, F., and White, C.I. (2005). Differing requirements for the Arabidopsis Rad51 paralogs in meiosis and DNA repair. Plant J. **41:** 533–545.

Boudolf, V., Inzé, D., and De Veylder, L. (2006). What if higher plants lack a CDC25 phosphatase? Trends Plant Sci. **11:** 474–479.

Branzei, D., and Foiani, M. (2010). Maintaining genome stability at the replication fork. Nat. Rev. Mol. Cell Biol. **11:** 208–219.

Brown, J.A., and Suo, Z. (2011). Unlocking the sugar "steric gate" of DNA polymerases. Biochemistry **50:** 1135–1142.

Bubeck, D., Reijns, M.A., Graham, S.C., Astell, K.R., Jones, E.Y., and Jackson, A.P. (2011). PCNA directs type 2 RNase H activity on DNA replication and repair substrates. Nucleic Acids Res. **39:** 3652–3666.

Cuéllar Pérez, A., Nagels Durand, A., Vanden Bossche, R., De Clercq, R., Persiau, G., Van Wees, S.C.M., Pieterse, C.M.J., Gevaert, K., De Jaeger, G., Goossens, A., and Pauwels, L. (2014). The non-JAZ TIFY protein TIFY8 from *Arabidopsis thaliana* is a transcriptional repressor. PLoS ONE **9:** e84891.

Cerritelli, S.M., and Crouch, R.J. (2009). Ribonuclease H: the enzymes in eukaryotes. FEBS J. **276:** 1494–1505.

Ciccia, A., and Elledge, S.J. (2010). The DNA damage response: making it safe to play with knives. Mol. Cell **40:** 179–204.

Clausen, A.R., Zhang, S., Burgers, P.M., Lee, M.Y., and Kunkel, T.A. (2013). Ribonucleotide incorporation, proofreading and bypass by human DNA polymerase δ. DNA Repair (Amst.) **12:** 121–127.

Cook, J.G. (2009). Replication licensing and the DNA damage checkpoint. Front Biosci (Landmark Ed) **14:** 5013–5030.

Cools, T., Iantcheva, A., Weimer, A.K., Boens, S., Takahashi, N., Maes, S., Van den Daele, H., Van Isterdael, G., Schnittger, A., and De Veylder, L. (2011). The *Arabidopsis thaliana* checkpoint kinase WEE1 protects against premature vascular differentiation during replication stress. Plant Cell **23:** 1435–1448.

Culligan, K., Tissier, A., and Britt, A. (2004). ATR regulates a G2-phase cell-cycle checkpoint in *Arabidopsis thaliana*. Plant Cell **16:** 1091–1104.

Culligan, K.M., Robertson, C.E., Foreman, J., Doerner, P., and Britt, A.B. (2006). ATR and ATM play both distinct and additive roles in response to ionizing radiation. Plant J. **48:** 947–961.

De Schutter, K., Joubès, J., Cools, T., Verkest, A., Corellou, F., Babiychuk, E., Van Der Schueren, E., Beeckman, T., Kushnir, S., Inzé, D., and De Veylder, L. (2007). Arabidopsis WEE1 kinase controls cell cycle arrest in response to activation of the DNA integrity checkpoint. Plant Cell **19:** 211–225.

Ferraro, P., Franzolin, E., Pontarin, G., Reichard, P., and Bianchi, V. (2010). Quantitation of cellular deoxynucleoside triphosphates. Nucleic Acids Res. **38:** e85.

Garcia, V., Bruchet, H., Camescasse, D., Granier, F., Bouchez, D., and Tissier, A. (2003). AtATM is essential for meiosis and the somatic response to DNA damage in plants. Plant Cell **15:** 119–132.

Gietz, D., St Jean, A., Woods, R.A., and Schiestl, R.H. (1992). Improved method for high efficiency transformation of intact yeast cells. Nucleic Acids Res. **20:** 1425.

Gonzalez, N., Hernould, M., Delmas, F., Gévaudant, F., Duffe, P., Causse, M., Mouras, A., and Chevalier, C. (2004). Molecular characterization of a WEE1 gene homologue in tomato (*Lycopersicon esculentum* Mill.). Plant Mol. Biol. **56:** 849–861.

Harper, J.W., and Elledge, S.J. (2007). The DNA damage response: ten years after. Mol. Cell **28:** 739–745.

Hartung, F., Suer, S., and Puchta, H. (2007). Two closely related RecQ helicases have antagonistic roles in homologous recombination and DNA repair in *Arabidopsis thaliana*. Proc. Natl. Acad. Sci. USA **104:** 18836–18841.

Hiller, B., Achleitner, M., Glage, S., Naumann, R., Behrendt, R., and Roers, A. (2012). Mammalian RNase H2 removes ribonucleotides from DNA to maintain genome integrity. J. Exp. Med. **209:** 1419–1426.

Ii, M., Ii, T., Mironova, L.I., and Brill, S.J. (2011). Epistasis analysis between homologous recombination genes in *Saccharomyces*

cerevisiae identifies multiple repair pathways for Sgs1, Mus81-Mms4 and RNase H2. Mutat. Res. **714:** 33–43.

Jefferson, R.A., Kavanagh, T.A., and Bevan, M.W. (1987). GUS fusions: beta-glucuronidase as a sensitive and versatile gene fusion marker in higher plants. EMBO J. **6:** 3901–3907.

Kim, N., Huang, S.N., Williams, J.S., Li, Y.C., Clark, A.B., Cho, J.E., Kunkel, T.A., Pommier, Y., and Jinks-Robertson, S. (2011). Mutagenic processing of ribonucleotides in DNA by yeast topoisomerase I. Science **332:** 1561–1564.

Kinner, A., Wu, W., Staudt, C., and Iliakis, G. (2008). Gamma-H2AX in recognition and signaling of DNA double-strand breaks in the context of chromatin. Nucleic Acids Res. **36:** 5678–5694.

Li, Y., Rosso, M.G., Strizhov, N., Viehoever, P., and Weisshaar, B. (2003). GABI-Kat SimpleSearch: a flanking sequence tag (FST) database for the identification of T-DNA insertion mutants in *Arabidopsis thaliana*. Bioinformatics **19:** 1441–1442.

Lopes, M., Cotta-Ramusino, C., Pellicioli, A., Liberi, G., Plevani, P., Muzi-Falconi, M., Newlon, C.S., and Foiani, M. (2001). The DNA replication checkpoint response stabilizes stalled replication forks. Nature **412:** 557–561.

Mannuss, A., Dukowic-Schulze, S., Suer, S., Hartung, F., Pacher, M., and Puchta, H. (2010). RAD5A, RECQ4A, and MUS81 have specific functions in homologous recombination and define different pathways of DNA repair in *Arabidopsis thaliana*. Plant Cell **22:** 3318–3330.

Miyabe, I., Kunkel, T.A., and Carr, A.M. (2011). The major roles of DNA polymerases epsilon and delta at the eukaryotic replication fork are evolutionarily conserved. PLoS Genet. **7:** e1002407.

Molinier, J., Ries, G., Bonhoeffer, S., and Hohn, B. (2004). Interchromatid and interhomolog recombination in *Arabidopsis thaliana*. Plant Cell **16:** 342–352.

Nick McElhinny, S.A., Kumar, D., Clark, A.B., Watt, D.L., Watts, B.E., Lundström, E.B., Johansson, E., Chabes, A., and Kunkel, T.A. (2010a). Genome instability due to ribonucleotide incorporation into DNA. Nat. Chem. Biol. **6:** 774–781.

Nick McElhinny, S.A., Watts, B.E., Kumar, D., Watt, D.L., Lundström, E.B., Burgers, P.M.J., Johansson, E., Chabes, A., and Kunkel, T.A. (2010b). Abundant ribonucleotide incorporation into DNA by yeast replicative polymerases. Proc. Natl. Acad. Sci. USA **107:** 4949–4954.

Ossowski, S., Schneeberger, K., Clark, R.M., Lanz, C., Warthmann, N., and Weigel, D. (2008). Sequencing of natural strains of *Arabidopsis thaliana* with short reads. Genome Res. **18:** 2024–2033.

Reijns, M.A.M., et al. (2012). Enzymatic removal of ribonucleotides from DNA is essential for mammalian genome integrity and development. Cell **149:** 1008–1022.

Ricaud, L., Proux, C., Renou, J.P., Pichon, O., Fochesato, S., Ortet, P., and Montané, M.H. (2007). ATM-mediated transcriptional and developmental responses to gamma-rays in Arabidopsis. PLoS ONE **2:** e430.

Rychlik, M.P., Chon, H., Cerritelli, S.M., Klimek, P., Crouch, R.J., and Nowotny, M. (2010). Crystal structures of RNase H2 in complex with nucleic acid reveal the mechanism of RNA-DNA junction recognition and cleavage. Mol. Cell **40:** 658–670.

Rydberg, B., and Game, J. (2002). Excision of misincorporated ribonucleotides in DNA by RNase H (type 2) and FEN-1 in cell-free extracts. Proc. Natl. Acad. Sci. USA **99:** 16654–16659.

Sambrook, J., Russell, D.W., and Sambrook, J. (2006). The Condensed Protocols from Molecular Cloning: A Laboratory Manual. (Cold Spring Harbor, NY: Cold Spring Harbor Laboratory Press).

Schneeberger, K., Ossowski, S., Lanz, C., Juul, T., Petersen, A.H., Nielsen, K.L., Jørgensen, J.E., Weigel, D., and Andersen, S.U. (2009). SHOREmap: simultaneous mapping and mutation identification by deep sequencing. Nat. Methods **6:** 550–551.

Schuermann, D., Fritsch, O., Lucht, J.M., and Hohn, B. (2009). Replication stress leads to genome instabilities in Arabidopsis DNA polymerase delta mutants. Plant Cell **21:** 2700–2714.

Sekiguchi, J., and Shuman, S. (1997). Site-specific ribonuclease activity of eukaryotic DNA topoisomerase I. Mol. Cell **1:** 89–97.

Sirbu, B.M., Couch, F.B., Feigerle, J.T., Bhaskara, S., Hiebert, S.W., and Cortez, D. (2011). Analysis of protein dynamics at active, stalled, and collapsed replication forks. Genes Dev. **25:** 1320–1327.

Sogo, J.M., Lopes, M., and Foiani, M. (2002). Fork reversal and ssDNA accumulation at stalled replication forks owing to checkpoint defects. Science **297:** 599–602.

Sorrell, D.A., Marchbank, A., McMahon, K., Dickinson, J.R., Rogers, H.J., and Francis, D. (2002). A WEE1 homologue from *Arabidopsis thaliana*. Planta **215:** 518–522.

Sparks, J.L., Chon, H., Cerritelli, S.M., Kunkel, T.A., Johansson, E., Crouch, R.J., and Burgers, P.M. (2012). RNase H2-initiated ribonucleotide excision repair. Mol. Cell **47:** 980–986.

Stein, H., and Hausen, P. (1969). Enzyme from calf thymus degrading the RNA moiety of DNA-RNA Hybrids: effect on DNA-dependent RNA polymerase. Science **166:** 393–395.

Sun, Y., Dilkes, B.P., Zhang, C., Dante, R.A., Carneiro, N.P., Lowe, K.S., Jung, R., Gordon-Kamm, W.J., and Larkins, B.A. (1999). Characterization of maize (*Zea mays* L.) Wee1 and its activity in developing endosperm. Proc. Natl. Acad. Sci. USA **96:** 4180–4185.

Swoboda, P., Gal, S., Hohn, B., and Puchta, H. (1994). Intrachromosomal homologous recombination in whole plants. EMBO J. **13:** 484–489.

Takahashi, N., Lammens, T., Boudolf, V., Maes, S., Yoshizumi, T., De Jaeger, G., Witters, E., Inzé, D., and De Veylder, L. (2008). The DNA replication checkpoint aids survival of plants deficient in the novel replisome factor ETG1. EMBO J. **27:** 1840–1851.

Van Leene, J., et al. (2007). A tandem affinity purification-based technology platform to study the cell cycle interactome in *Arabidopsis thaliana*. Mol. Cell. Proteomics **6:** 1226–1238.

Van Leene, J., Witters, E., Inzé, D., and De Jaeger, G. (2008). Boosting tandem affinity purification of plant protein complexes. Trends Plant Sci. **13:** 517–520.

Van Leene, J., et al. (2010). Targeted interactomics reveals a complex core cell cycle machinery in *Arabidopsis thaliana*. Mol. Syst. Biol. **6:** 397, 12.

Wang, J.C. (2002). Cellular roles of DNA topoisomerases: a molecular perspective. Nat. Rev. Mol. Cell Biol. **3:** 430–440.

Williams, J.S., and Kunkel, T.A. (2014). Ribonucleotides in DNA: origins, repair and consequences. DNA Repair (Amst.) **19:** 27–37.

Williams, J.S., Clausen, A.R., Nick McElhinny, S.A., Watts, B.E., Johansson, E., and Kunkel, T.A. (2012). Proofreading of ribonucleotides inserted into DNA by yeast DNA polymerase ϵ. DNA Repair (Amst.) **11:** 649–656.

Williams, J.S., Smith, D.J., Marjavaara, L., Lujan, S.A., Chabes, A., and Kunkel, T.A. (2013). Topoisomerase 1-mediated removal of ribonucleotides from nascent leading-strand DNA. Mol. Cell **49:** 1010–1015.

Willis, N., and Rhind, N. (2009). Regulation of DNA replication by the S-phase DNA damage checkpoint. Cell Div. **4:** 13.

Wu, T.D., and Nacu, S. (2010). Fast and SNP-tolerant detection of complex variants and splicing in short reads. Bioinformatics **26:** 873–881.

Zegerman, P., and Diffley, J.F.X. (2009). DNA replication as a target of the DNA damage checkpoint. DNA Repair (Amst.) **8:** 1077–1088.